This is the accepted manuscript made available via CHORUS. The article has been published as:

Stabilization of highly polarized PbTiO_{3} nanoscale capacitors due to in-plane symmetry breaking at the interface

Miguel Angel Méndez Polanco, Ilya Grinberg, Alexie M. Kolpak, Sergey V. Levchenko, Christopher Pynn, and Andrew M. Rappe

Phys. Rev. B **85**, 214107 — Published 7 June 2012

DOI: 10.1103/PhysRevB.85.214107

Stabilization of highly-polarized $PbTiO_3$ nanocapacitors due to in-plane symmetry-breaking at the interface

Miguel Angel Méndez Polanco, Ilya Grinberg, Alexie M. Kolpak,*
Sergey V. Levchenko,† Christopher Pynn, and Andrew M. Rappe‡
The Makineni Theoretical Laboratories, Department of Chemistry,
University of Pennsylvania, 231 S. 34th Street Philadelphia, Pennsylvania 19104–6323, USA

Stable ferroelectric (FE) phases in nanometer-thick films would enable ultra-high density and fast FE field effect transistors (FeFETs), and the stability of ferroelectricity in ultrathin films has been under intense theoretical and experimental investigation. Here we predict, using density functional theory calculations, that the low-energy epitaxial $PbTiO_3$ (001)/Pt interface strengthens the electrode-oxide bonds by breaking in-plane symmetry and stabilizes a ground state with enhanced polarization in sub-nanometer oxide films, with no critical-size limit. Additionally, we show that such enhancement is related to large work function differences between the P^- and P^+ $PbTiO_3$ surfaces, which gives rise to a net polarizing field in the oxide.

PACS numbers: 85.50.-n, 68.35.-p, 73.30.+y, 77.22.Ej

I. INTRODUCTION

Bulk ferroelectricity has multiple applications in technology, from actuators and sensors to catalysis and information storage[1–3]. In particular, due to the convenient control of polarization ($\vec{P}$) orientation with applied electric field, ferroelectricity can be useful in non-volatile memory and other information processing devices. However, in these systems, the small thickness of the film gives rise to a depolarizing field ($\varepsilon_{\rm dep}$) caused by uncompensated surface charges[4]. In the case when the top and bottom electrodes are similar, and the potential drop in the material is smaller than the band gap, $\varepsilon_{\rm dep}$ is given by:

$$\varepsilon_{\rm dep} = -2\frac{\lambda_{\rm eff}}{d\,\epsilon_0}P \qquad (1)$$

where $\lambda_{\rm eff}$ is the *effective* screening length of the system, and d and P are the thickness and polarization of the FE film, respectively[5]. The $\varepsilon_{\rm dep}$ becomes stronger as the thickness of the sample is decreased and can suppress polarization entirely. Optimal ways to overcome this deleterious effect and improve FE stability of films have been the focus of intense theoretical and experimental study[4–20]. It has been shown that the details of the chemical bonding at the interface play a critical role in determining the effectiveness of the screening and properties of films such as interface-induced polarization, ease of polarization switching and FE stability in perovskite-based capacitors[18,20]. In addition, charge compensation by adsorbed molecules is also highly effective; it has been demonstrated to govern the magnitude and sign of the surface potential on FE surfaces and to stabilize ferroelectricity in ultrathin films and nanowires[12,17,21,22], providing further evidence for the important role played by interfacial chemical bonding in determining FE stability.

Consideration of an idealized capacitor device consisting of a perovskite oxide insulator sandwiched between metal electrodes[7] demonstrates that symmetry breaking polarization creates different chemical interactions at the positive and negative oxide/electrode interfaces. This gives rise to a difference in the work function at the two surfaces of the FE slab, which is of crucial importance for the screening of the polarization surface charge.[13,23] However, while previous theoretical studies have examined the effects of interface interactions, they have primarily considered changes in the oxide structure perpendicular to the interface. Consequently, little is currently known about how atomic scale rearrangements *parallel* to the interface — for example, polarization-induced surface reconstructions or shifts of the metal layer with respect to the underlying oxide registry — can affect the behavior of FE capacitors. In this work, we use density functional theory calculations to elucidate the role of the latter in the classic $Pt/PbTiO_3/Pt$ metal/oxide nanocapacitors, exploring different registries of Pt atoms on the $PbTiO_3$ surface and optimizing all degrees of freedom. We find that the lowest energy interface structure deviates significantly from that considered in previous works, exhibiting a net *polarizing* field that increases P with decreasing film thickness, in contrast to the expected behavior.

Our analysis demonstrates that although the lateral relaxation reduces P enhancement with respect to the in-plane symmetric structures, it plays a vital role by creating more favorable bonding at the interface. This lowers the energy of the polarized state relative to the nonpolar state, making it the global minimum on the potential energy surface. These two factors (polarization enhancement and favorable bonding) are both important to attain globally stable FE polarization in an oxide thin film.

II. METHODOLOGY

We performed density functional theory (DFT) calculations using the PBEsol exchange-correlation functional[24] as implemented in the Quantum Espresso[25] DFT

DRAFT

code. The PBEsol functional was shown by Perdew and collaborators to describe solids and surfaces accurately, and it recently has been used successfully to study $PbTiO_3$ bulk and thin films.[26]

A supercell slab method was used to describe the different FE thin film capacitors. The supercells consist of a $PbTiO_3$ oxide region sandwiched by Pt electrodes, with approximately 18 Å of vacuum separating images. The atoms were represented by norm-conserving pseudopotentials[27] generated using the code OPIUM[28] with a plane-wave cutoff of 50 Ry. We performed the structural relaxation at the theoretical in-plane lattice constant of tetragonal $PbTiO_3$, attaining an optimized structure when forces are lower than 10 meV/Å on each atom. In addition to upper and lower interfaces with equivalent registries, we studied inequivalent registries of Pt electrodes on (001) $PbTiO_3$ FE surfaces. Figures depicting the different capacitor arrangements were created using the VESTA software.[29] In the presence of symmetry-breaking polarization, we consider four possible interfaces: Top/$P^- \cdots P^+$/Top; Top/$P^- \cdots P^+$/Hollow; Hollow/$P^- \cdots P^+$/Top; and Hollow/$P^- \cdots P^+$/Hollow (hereafter labeled as **TT, TH, HT** and **HH**, respectively). Figure 1 depicts the naming scheme we use for the studied systems. Here, "Top" refers to registries in which the Pt atoms are directly above the oxide surface atoms (Pb and O), while Pt atoms in the "Hollow" registry are over unoccupied lattice sites on the surface.

We assess the stability of each of the different arrangements by comparing the energy per $PbTiO_3$ unit cell of a given polar structure with the paraelectric (PE) state in the TT registry:

$$\Delta E = \frac{(E_{\mathrm{FE}} - E_{\mathrm{PE^{TT}}})}{N_{\mathrm{PbTiO_3\ unit-cell}}} \qquad (2)$$

Analysis of the density of states (DOS) per PTO layer in the capacitors, Fig. 2, shows that the metallic behavior is localized at the interface, with exponential decay of the metallic states within the oxide region. Therefore, metallic layers at the interface are attributed to the chemical bonding between atoms, *e.g.* localized charge transfer at the interfaces; this effect is confined to the interface layers, and the bulk PTO layers remain insulating. This is in agreement with previous studies of the AO/Pt interfaces,[13,14,18,23,26] and it means that our system exhibits proper band alignment of the metal and oxide[30]. Also, supporting this conclusion, the cation displacements with respect to oxygen atoms in each layer (rumplings, Fig. 2c) show uniform enhancement of the polarization throughout the oxide film[23,30] for all the capacitor systems.

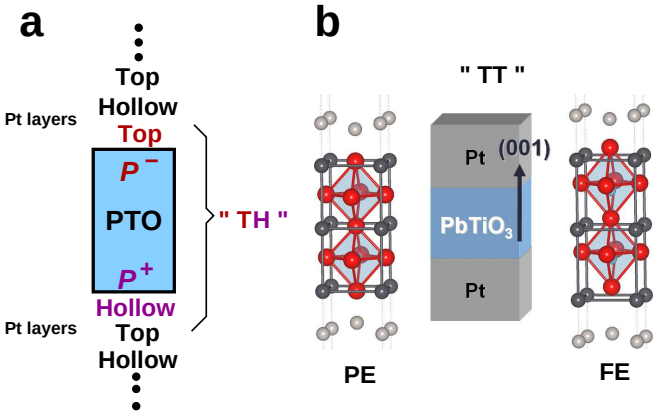

FIG. 1. Nomenclature convention for the nanocapacitor systems. Names are based on the atomic arrangements at the interfaces, and Pt layers are assumed to follow FCC (001) stacking. **a**, Schematic diagram and name of one of the interfaces studied here. **b**, Model of relaxed TT capacitors in the PE and FE state. For clarity, only the interfacial Pt-electrode atoms are shown. Color labeling (online version): Pb = dark grey, Ti = cyan, O = red, and Pt = light grey.

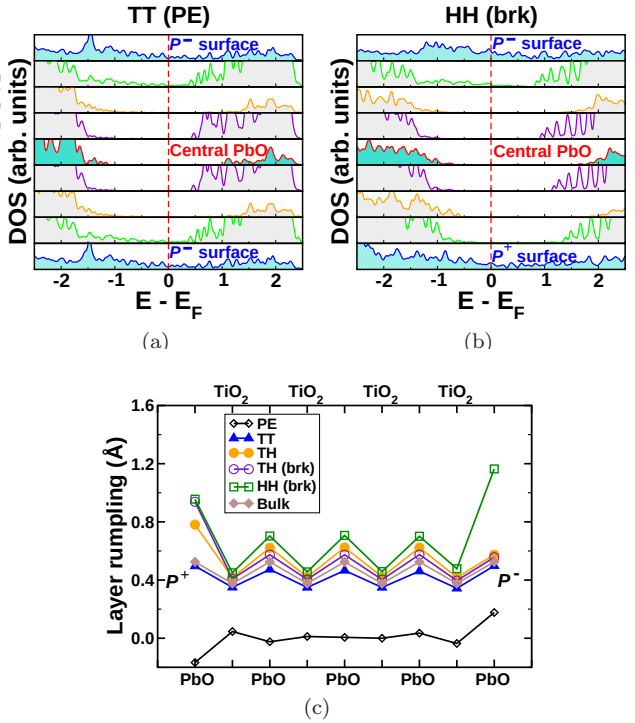

FIG. 2. Density of states (DOS) in each oxide layer for the capacitor systems. The interfaces and central layer are labeled in the figure. Shown here are the DOS for the (a) TT-PE and (b) HH_{brk}, 4 unit-cell PTO capacitors, note the local insulating character of the inner layers of the oxide film. (c) Absolute value of the layer rumpling (Cation(z) - Oxygen (z) displacement in the z-axis).

DRAFT

III. RESULTS AND DISCUSSIONS

A. Inequivalent Pt electrodes under the in-plane symmetry constraint

We first examined the structures and energetics of the various $Pt/PbTiO_3/Pt$ capacitors under the constraint of bulk-like lateral ionic coordinates. For paraelectric (PE) $PbTiO_3$, the TT interface registry that was used in previous theoretical studies is energetically preferred. For polar $PbTiO_3$ films, however, the polarization of the oxide influences the energetics of Pt on the (001) surfaces so that the top sites are preferred for the P^- surface while the hollow sites are preferred on the P^+ surface. We find that epitaxial Pt electrodes in the TH registry stabilize a polar $PbTiO_3$ structure relative to the PE state. This is in contrast with previous studies[14] that found that at the theoretical lattice constant, the PE state is more stable for $PbTiO_3$ films less than 6 unit-cells thick. The HH and HT structures are least favorable and are metastable local minima with high energy. The strong enhancement of FE polarization in one particular direction (TH) while disfavoring the opposite polarization (HT), is analogous to the findings of Umeno *et al.* [19] for capacitors with an asymmetric combination of electrodes, $SrRuO_3/PbTiO_3/Pt$. Since our system has compositionally equivalent electrodes, our results emphasize the importance of the local atomic rearrangement at the interface.

Analysis of the structural differences between the T and H interfaces at the P^+ and P^- surfaces sheds light on the $Pt/PbTiO_3$ interface energetics. In the T registry, one half of the Pt atoms sit on top of the Pb atoms and one half are on top of the O atoms. For the P^+ surface, the Pb atoms lie higher than the surface O atoms, which relax inward. This makes the Pt-Pb distances short and Pt-O distances long, indicating weak Pt-O bonds. Thus, for the Top/P^+ case, one half of the Pt atoms are only weakly bound to the oxide surface. In contrast, for the H registry each Pt atom has two Pb and two O nearest neighbors. Consequently in the H/P^+ case all Pt atoms can form strong Pt-Pb bonds, making this interface preferred over T/P^+ and stabilizing the TH relative to the TT and PE (TT) capacitors.

The opposite preference is found for the P^- surface. For the T/P^- interface, the positively charged Pt atoms that form ionic bonds with surface O are located far away from the positively charged Pb atoms, minimizing the electrostatic repulsion. For the H/P^- surface, the short bonds between Pt and O would bring the positively charged Pt atoms close to the Pb cations and give rise to a strong electrostatic repulsion. Instead, the O atoms are extracted from the $PbTiO_3$ surface and move up close to the Pt layer. As we show later, this is a key contribution for P enhancement in films with respect to the bulk. However, the breaking of the O-Ti and O-Pb bonds raises the energy of the H/P^- configuration, destabilizing HH relative to the TH and TT configurations.

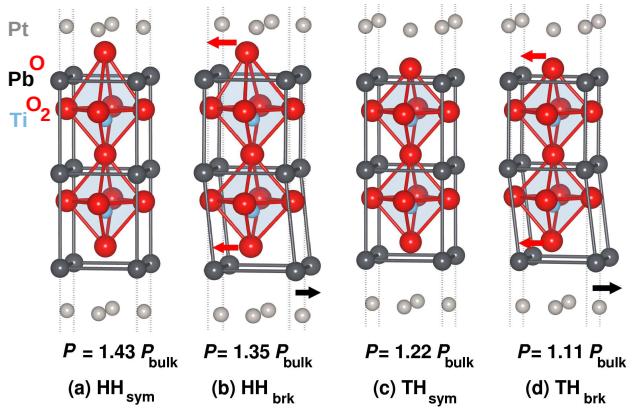

FIG. 3. Fully relaxed two-unit cell $Pt/PbTiO_3/Pt$ nanocapacitors. (a) HH_{sym}, (b) HH_{brk}, (c) TH_{sym} and (d) TH_{brk}, only the interfacial Pt atoms are shown for clarity. The predominant structural changes are the displacement of the atoms at the P^+ interface for TH, and at the P^- interface for HH, as indicated by arrows. The estimated polarization with respect to that of bulk is shown for each configuration.

B. Fully-relaxed, broken symmetry interfaces

Interestingly, our calculations show that relaxation of all degrees of freedom for the nanocapacitors leads to an in-plane symmetry-breaking at the interfaces, resulting in a large stabilization of the otherwise metastable HH capacitor. Figure 3 depicts the lowest-energy (panels b and d), broken-symmetry structures along with their in-plane symmetry preserved counterparts. We labeled the two lower-energy structures with broken in-plane symmetry as TH_{brk} and HH_{brk}. Due to in-plane relaxation, the high-energy HH_{sym} structure is stabilized by 250 meV/$PbTiO_3$-UC as it evolves into HH_{brk}, which is the lowest-energy arrangement, approximately 150 meV/$PbTiO_3$-UC more stable than the paraelectric TT capacitor. In contrast, the energy of the TH arrangement is only lowered by approximately 10 meV/$PbTiO_3$-UC when in-plane symmetry breaking is allowed (Table I).

Our findings imply that the TT in-plane–constrained structure previously considered as a model of the oxide/metal electrode interface is only a saddle point and not a local minimum of the full potential energy surface.

Comparison of the energy difference and structural features of the symmetric and asymmetric arrangements shows that the oxygen tilting occurring at the P^- interface makes the largest impact in the stabilization of broken-symmetry interfaces. For the P^- surface, the interfacial oxygen atoms move by ≈ 0.3 Å, making short 2.0 Å bonds with one of their Pt neighbors, while the oxygen atoms in the TiO_2 layer stay nearly in their symmetric position. This atomic rearrangement favors the stability of the capacitor, as it creates stronger Pt-O bonds and compensates for the weakened bonds between the surface O and Pb atoms. On the other side of the film, the Pb

PREPRINT

System	ΔE (meV/UC)	ϵ_{FE} Field (mV/Å)			Δ (mV)		λ (Å)
	4 PTO/5 Pt	Free slab	Thomas-Fermi	DFT	Δ_1	Δ_2	Calculated
TT_{sym}	-50.0	-123.8	-10.2	-11.6	-1680	-2740	0.040
TH_{sym}	-129.0	-105.4	15.4	23.8	-1470	-2750	0.064
TH_{brk}	-136.0	-104.6	11.5	17.8	-1390	-2800	0.068
HH_{sym}	+106.4	-57.7	64.0	61.5	-1020	-3850	0.134
HH_{brk}	-151.4	-56.7	42.1	44.9	-890	-3810	0.131

TABLE I. Energetics and electrostatic potential data. Energy differences per unit cell with respect to the four unit-cell PE-PTO, 5TT5 capacitor. E fields (mV/Å) are calculated from DFT and our modified Thomas-Fermi screening model. Potential drops (mV), Δ_1 and Δ_2, are obtained from DFT for a frozen free-standing film. The field inside the FE region in the capacitor system is strongly influenced by $\Delta_2 - \Delta_1$: The larger this difference is, the more positive the net ϵ_{FE} field in the capacitor is.

atoms on the P^+ surface move laterally in the xy-plane, decreasing the Pb-O distance by approximately 0.3 Å, in conjunction with a small oxygen tilt ($\approx 2.5°$).

C. Net polarizing field and Polarization enhancement in PTO films

To study the screening in the nanocapacitor, we decompose the system into its oxide and electrode components.[31] Analysis of the planar-averaged electronic charge density normal to the surface ($\rho(z) = \int dx \int dy \rho(x,y,z)/A_{xy}$, where A_{xy} is the cross-section area of the cell)[6,32] for the capacitors (Fig. 4) shows that it is essentially just a sum of the charge densities of the bare oxide and Pt electrode fixed in their respective capacitor geometries. Therefore, the screening in the nanocapacitor can be modeled as the metal electrode screening of the electrostatic potential profile of the bare oxide in the nanocapacitor geometry.

Analysis of the $PbTiO_3$ cation displacements shows that P values for the nanocapacitors previously presented in Fig. 3 are greater than those of bulk $PbTiO_3$.[33] This is in contrast with the TT_{sym} structure, for which P is reduced compared to the bulk value. A comparison of HH and TH P magnitudes shows that $P_{HH} > P_{TH}$ for both the in-plane constrained and the broken symmetry structures.

The enhancement of P above the bulk value suggests the presence of a polarizing field. To confirm this and to understand the origin of the enhancement, we plot the macroscopic-averaged electrostatic potential of each capacitor and compare it to the potential of their corresponding *bare* $PbTiO_3$ film (removing all the Pt atoms from the calculation and freezing the $PbTiO_3$ ions in the relaxed geometry of the $Pt/PbTiO_3/Pt$ heterostructure). The electrostatic potential profiles clearly show that the enhanced P values of the nanocapacitors are due to a net polarizing field in the film, as evidenced by the change in the sign of the slope in the presence of electrodes with respect to the frozen free-standing film (Figure 5). For instance, in the case of the TT_{sym} geometry the net remnant field is depolarizing (the frozen bare oxide and the capacitor have the same sign of the slope in the electrostatic potential); although drastically

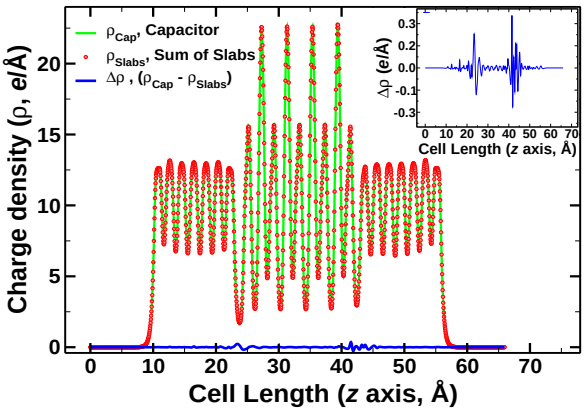

FIG. 4. Electron charge density along z in the unit cell ($\rho(z)$ in units of e/Å/(cell cross-section). DFT-obtained electronic charge density for the TT capacitor system compared with the sum of the isolated metal and oxide charge densities calculated separately frozen in the respective capacitor geometries. The small difference between the two (inset) means that the capacitor systems can nearly be split into their individual isolated oxide and metal components.

DRAFT

reduced to ≈ -10 mV/Å, it is not eliminated entirely. On the other hand, for HH_{brk}, for example, we find the appearance of a *polarizing* field of ≈ 40 mV/Å (note the change of the sign of the slope).

The differences in the screening properties of the nanocapacitors can be directly related to the differences in the work functions on the positive and negative bare-$PbTiO_3$ surfaces. Previous work[13] has shown that for polar $PbTiO_3$, this difference is the variation between the two vacuum potentials for the frozen bare slab (Δ_2) and it is greater than the potential drop inside the film (Δ_1), see Fig. 5a, b. Thus, screening of the difference in the work functions at the two surfaces in the oxide by the electrodes can overscreen the potential drop due to polarization and create a polarizing field. Similarly, the importance of Schottky barrier heights (SBH) for the screening in ferroelectric oxides has also been analyzed in detail by Stengel *et al.*[23] using constrained displacement-field calculations. Examination of the electrostatic potential plots shows that for the bare slab in the HH_{brk} geometry, the work function difference is larger (-3.8 V for HH_{brk}

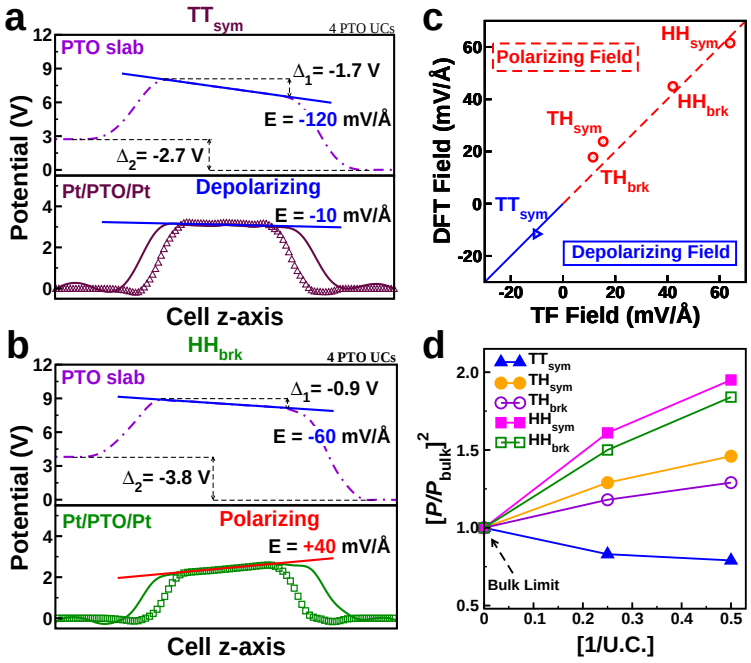

FIG. 5. Macroscopic averaged electrostatic potential ($\bar{V}(z)$) plots. **a, b** Potential in the frozen free-standing $PbTiO_3$ film (upper panel, dot-dashed line), their corresponding capacitors (solid line) and potential from our Thomas-Fermi model (open symbols). Polarization points ($P^+ \leftarrow P^-$) in the plot. A net polarizing field can develop in the oxide film, indicated by the flip in the sign of the slope, if the screening of Δ_2 overscreens Δ_1, as in the case of HH_{brk}. **c** A comparison of the electric field calculated values in the $PbTiO_3$ films (ε_{FE}) for all registries, shows that the Thomas-Fermi model accurately reproduces the trends found by DFT, as long as $\Delta_2 - \Delta_1$ is included. **d** Relationship between P^2 and the inverse $PbTiO_3$ film thickness. The TT capacitor shows decreasing P as film thickness is decreased. By contrast, the low-energy broken-symmetry structures, follow the opposite trend. Hence, there is no intrinsic critical size limit for these capacitors, due to the broken symmetry and enhanced screening.

DRAFT

vs. -2.7 V for TT_{sym}). This is due to the much stronger PbO surface rumpling at the HH interface. The separation between the O and the Pb atoms is greater for the HH interface, with the O atom rising out of the surface by ≈ 0.7 Å more than in the TT case. This makes the electrostatic potential more repulsive for electrons and increases the work function difference magnitude.

The screening can be described by a standard depolarizing field equation, generalized to the case of different work functions at the surfaces of the FE. In this case, the net electric field inside the FE is given by:

$$\varepsilon_{FE} = \frac{P}{\epsilon_0}\left(\frac{2\lambda}{d}\right) + \frac{(\Delta_2 - \Delta_1)}{d}\left(1 - \frac{2\lambda}{d}\right) \qquad (3)$$

Inspection of Eq. 3 suggests that a large $\Delta_2 - \Delta 1$ would play a crucial role in the screening and can result in a polarizing field, equivalent to a negative *effective* screening length in Eq. 1. We use our DFT-computed values of ε_{FE}, P, Δ_1 and Δ_2 to solve Eq. 3 for the λ values in the different capacitor arrangements. The corresponding values are shown in Table I and range from 0.04 Å to 0.13 Å. Note that for the TT_{sym} interface, which most closely resembles the bulk $PbTiO_3$ and Pt structures, the λ value is the smallest, while the HH interfaces exhibit values that are three times larger than those. According to the classic theory, which assumes equivalent electrostatic potentials at the P^- and P^+ surfaces of the oxide, the poorer screening at the HH interface would lead to larger depolarizing field, in stark contrast to the strong *polarizing* field found by DFT calculations.

To show that the combination of simple metallic screening and a large difference in the surface electrostatic potential drops at the P^- and P^+ surfaces ($\Delta_2 - \Delta_1$) in the FE slab is sufficient to account for the results found by our DFT calculations, we use a simple Thomas-Fermi model for the electrode electrons in the nanocapacitor. The Thomas-Fermi equation is solved iteratively to obtain the total electrostatic potential due to screening by the free electrons in the electrodes. The nanocapacitor electrostatic potentials, and their associated ε_{FE}, are obtained from direct DFT calculations and from the Thomas-Fermi model applied to the DFT-extracted bare oxide potentials (Fig. 5a, b and Table I). The close quantitative agreement between these results (Fig. 5c) indicates that our model can capture the essential features of all the charge compensation mechanisms that contribute to the stability of ferroelectricity in ultrathin films, and thus highlights the importance of the $\Delta_2 - \Delta_1$ difference as the main contributor to the interface-induced modifications in the depolarizing field. Furthermore, our results provide a straightforward guide-

line for stabilizing FE in ultrathin films: since Δ_2 is created by vertical separation between the surface cations and anions, the strongest reduction of the depolarizing field will occur for interfaces that create larger rumpling in the surface layer of the FE oxide.

The presence of enhanced polarization is not sufficient on its own to guarantee that ferroelectricity is energetically stable relative to the PE phase. As shown in Fig. 5d, P^2 scales as $1/d$ reaching the highest values for the ultrathin film systems. This trend shows that P enhancement for the $Pt/PbTiO_3/Pt$ capacitors in the TH and HH-related systems, in principle, has no critical size limit. However, a comparison of the in-plane constrained and relaxed nanocapacitor energies and P values shows that there are two criteria for stability in ultrathin perovskite films. First, the electrode must screen the surface charges well enough to remove the depolarizing field. This makes the FE state a local minimum on the potential energy surface. Such a minimum could still be higher in energy than the PE state due to a less favorable bonding at the interfaces. Hence, the second requirement is that the bonding energy of the metal-oxide interface for the polarized state must be equal to or greater than the metal-oxide bonding energy of the paraelectric state. That is, in films where the FE state is the global minimum, an interface with larger vertical rumplings reduces the depolarizing field while in-plane relaxation provides the favorable interface chemistry that lowers the energy of the rumplings.

To illustrate these criteria, consider the HH_{sym} and the HH_{brk} nanocapacitors. In the HH_{sym} system, the overscreening leads to a 37% increase in P for the FE state. Nonetheless, the metal-oxide bonding is significantly weaker than for the paraelectric case, making the HH_{sym} FE state a high-energy local minimum. When the in-plane symmetry is broken, the screening is not quite as efficient, leading to a P enhancement of only 24% for the HH_{brk} structure. However, the metal-oxide bonding is stronger. This lowers the energy of the HH_{brk} nanocapacitor making it the global minimum on the potential energy surface.

To describe these two criteria in the language of the Landau-Ginzburg-Devonshire (LGD) theory, we introduce additional order parameters to represent the surface deformation and the bonding interaction at the interface[34] and write:

$$U_{tot} = n\left(-\frac{1}{2}AP^2 + \epsilon_{FE}P + \frac{1}{4}BP^4\right) + aS_{top} + \frac{1}{2}bS_{top}^2 - aS_{bot} + \frac{1}{2}bS_{bot}^2 - kS_{top}P - kS_{bot}P \quad (4)$$

where U_{tot} is the total energy of the system, n is the thickness of the oxide film in unit cells, P is the polarization of the oxide, S_{top} and S_{bot} are the surface order parameters relating to the structural changes at the surface due to the metal-oxide bonding and A, B, a, b and k are constants parameterizing the oxide ferroelectricity, surface bonding and the interplay between P and structural changes due to the metal-oxide bonding. The presence of the additional order parameters makes the potential energy surface complex and allows for the existence of metastable states.

Minimizing the energy with respect to all three order parameters shows that three minima are present on the potential energy surface. For a paraelectric state, $S_{top} = -S_{bot} = -a/b$; here, the interfaces are symmetrically deformed, as we indeed find for the PE capacitor where both surfaces are locally P^- with the oxygen atoms sticking out from the surface. For the FE state, the surface deformation will be different at the two surfaces, as found by DFT calculations, with one surface forced away from its preferred state by the coupling of the surface atom displacements to the film P.

To illustrate the impact of the oxide-metal bonding on the relative stability of the FE and PE states and the critical thickness, we compare the energy of the PE state and the energy of the FE state at $P = P_0$ (polarization of the oxide bulk). For convenience, we use a case where the constant k that scales the strength of the coupling between the surface order parameter and the bulk P is such that $kP_0 = a$.
The energy of the PE state is given by

$$U_{tot}^{PE} = 2U_{int}^{0} = -a^2/b \quad (5)$$

For the FE state with $P = P_0$ and $kP_0 = a$, S_{top} and S_{bot} are 0 and $2a/b$ respectively. In this case, the interface energy for the top and bottom surfaces is 0 and the energy of the system is given by:

$$U_{tot}^{FE} = nU_{bulk}^{FE} - 2a^2/b \quad (6)$$

where U_{bulk}^{FE} is the energy due to ferroelectric polarization in the oxide unit cell at $P = P_0$.
Setting the PE and FE cases to the same energy and solving for n, we get:

$$n_{crit} = (a^2/b)/U_{bulk}^{FE} \quad (7)$$

Thus, due to the effect of the interface, it is possible to have a high n_{crit}, even for the case where the depolarizing field has been eliminated by a full compensation of the surface charge or even in the presence of a polarizing field. We emphasize that the n_{crit} here is the critical thickness at which the FE state is the ground state of the system, not the one at which the P can be metastable but only as a local minimum, higher in energy than the PE state. These effects are independent of the depolarizing field, as illustrated by the comparison between the HH_{sym} and the HH_{brk} systems above.

IV. CONCLUSIONS

We conclude that even for simple surfaces with bulk stoichiometry, energy minimization with respect to lat-

DRAFT

eral degrees of freedom is necessary to find the correct ground state structure of FE/metal nanocapacitors. We find that the ground state for the classic $Pt/PbTiO_3/Pt$ systems exhibits a strong polarization enhancement due to the polarizing field. This leads to P *increase* as the film size *decreases*. There are two requirements for stable, FE $PbTiO_3$ ultrathin films with no critical size limit: 1) overscreening of depolarizing field, caused by strong surface rumpling and large oxide work function differences; this allows a minimum energy-state with $P > 0$ to exist, and 2) favorable chemical bonding at the interface, allowed by ionic in-plane relaxation, which then ensures that the FE state is a global minimum.

We hope that our findings will encourage development of experimental techniques that allow for a better controlled epitaxial growth of FE films and the use of characterization techniques such as X-ray photoelectron diffraction (XPD), low temperature Raman scattering using UV illumination or grazing incidence X-ray diffraction (GIXD) to reveal surface structure features, *i. e.* intra-cell atomic-displacement distributions or symmetry-lowering due to surface O-Ti bond tilts and to advance the understanding of the impact of surface structure on the screening properties of the interface.

V. ACKNOWLEDGEMENTS

MAMP was supported by the DoE Office of Basic Energy Sciences, under grant number DE-FG02-07ER15920. IG was supported by the Office of Naval Research, under grant N00014-11-1-0578. AMR was supported by the Air Force Office of Scientific Research, Air Force Materiel Command, USAF, under Grant No. FA9550-10-1-0248. Computational support was provided by the HPCMO of the US DoD. We thank Seungchul Kim, Wissam Al-Saidi, Jonathan Spanier and Javier Junquera for fruitful discussions.

DRAFT

* Current address: Dept. of Materials Science and Engineering, Massachusetts Institute of Technology
† Current address: Fritz-Haber-Institut der Max-Planck-Gesellschaft, Theory Department, Faradayweg 4-6 D-14195 Berlin-Dahlem, Germany
‡ To whom correspondence should be addressed: rappe@sas.upenn.edu

[1] M. W. Finnis, J. Phys.: Condens. Matter **8**, 5811 (1996).
[2] M. Dawber, K. M. Rabe, and J. F. Scott, Rev. Mod. Phys. **77**, 1083 (2005).
[3] C. R. A. Catlow, S. A. French, A. A. Sokol, M. Alfredsson, and S. T. Bromley, Faraday Discuss. **124**, 185 (2003).
[4] I. P. Batra and B. D. Silverman, Solid State Commun. **11**, 291 (1972).
[5] R. R. Mehta, B. D. Silverman, and J. T. Jacobs, J. Appl. Phys. **44**, 3379 (1973).
[6] J. Junquera and P. Ghosez, Nature **422**, 506 (2003).
[7] M. Dawber, P. Chandra, P. B. Littlewood, and J. F. Scott, J. Phys.: Condens. Matter **15**, L393 (2003).
[8] C. Ederer and N. A. Spaldin, Phys. Rev. Lett. **95**, 257601 (2005).
[9] K. M. Rabe, Current Opinion in Solid State and Materials Science **9**, 122 (2005), ISSN 1359-0286.
[10] L. Despont, C. Koitzsch, F. Clerc, M. G. Garnier, P. Aebi, C. Lichtensteiger, J.-M. Triscone, F. J. Garcia de Abajo, E. Bousquet, and P. Ghosez, Phys. Rev. B **73**, 094110 (2006).
[11] G. Gerra, A. K. Tagantsev, N. Setter, and K. Parlinski, Phys. Rev. Lett. **96**, 107603 (2006).
[12] D. D. Fong, A. M. Kolpak, J. A. Eastman, S. K. Streiffer, P. H. Fuoss, G. B. Stephenson, C. Thompson, D. M. Kim, K. J. Choi, C. B. Eom, I. Grinberg, and A. M. Rappe, Phys. Rev. Lett. **96**, 127601 (2006).
[13] N. Sai, A. M. Kolpak, and A. M. Rappe, Phys. Rev. B Rapid Comm. **72**, 020101(R) (2005).
[14] Y. Umeno, B. Meyer, C. Elsässer, and P. Gumbsch, Phys. Rev. B **74**, 060101R (2006).
[15] D. G. Schlom, L.-Q. Chen, C.-B. Eom, K. M. Rabe, S. K. Streiffer, and J.-M. Triscone, Annual Review of Materials Research **37**, 589 (2007).
[16] G. Gerra, A. K. Tagantsev, and N. Setter, Phys. Rev. Lett. **98**, 207601 (May 2007).
[17] R. V. Wang, D. D. Fong, F. Jiang, M. J. Highland, P. H. Fuoss, C. Thompson, A. M. Kolpak, J. A. Eastman, S. K. Streiffer, A. M. Rappe, and G. B. Stephenson, Phys. Rev. Lett. **102**, 047601 1 (2009).
[18] M. Stengel, D. Vanderbilt, and N. A. Spaldin, Nat Mater **8**, 392 (2009).
[19] Y. Umeno, J. M. Albina, B. Meyer, and C. Elsässer, Phys. Rev. B **80**, 205122 (Nov 2009).
[20] A. M. Kolpak, F. J. Walker, J. W. Reiner, Y. Segal, D. Su, M. S. Sawicki, C. C. Broadbridge, Z. Zhang, Y. Zhu, C. H. Ahn, and S. Ismail-Beigi, Phys. Rev. Lett. **105**, 217601 (Nov 2010).
[21] S. V. Kalinin and D. A. Bonnell, Nano Lett. **4**, 555 (2004).
[22] J. E. Spanier, A. M. Kolpak, J. J. Urban, I. Grinberg, L. Ouyang, W. S. Yun, A. M. Rappe, and H. Park, Nano Lett. **6**, 735 (2006).
[23] M. Stengel, D. Vanderbilt, and N. A. Spaldin, Phys. Rev. B **80**, 224110 (Dec 2009).
[24] J. P. Perdew, A. Ruzsinszky, G. I. Csonka, O. A. Vydrov, G. E. Scuseria, L. A. Constantin, X. Zhou, and K. Burke, Phys. Rev. Lett. **100**, 136406 (Apr 2008).
[25] P. Giannozzi, S. Baroni, N. Bonini, M. Calandra, R. Car, C. Cavazzoni, D. Ceresoli, G. L. Chiarotti, M. Cococcioni, I. Dabo, A. D. Corso, S. de Gironcoli, S. Fabris, G. Fratesi, R. Gebauer, U. Gerstmann, C. Gougoussis, A. Kokalj, M. Lazzeri, L. Martin-Samos, N. Marzari, F. Mauri, R. Mazzarello, S. Paolini, A. Pasquarello, L. Paulatto, C. Sbraccia, S. Scandolo, G. Sclauzero, A. P. Seitsonen, A. Smogunov, P. Umari, and R. M. Wentzcovitch, J. Phys.: Condens. Matter **21**, 395502 (2009).
[26] W. A. Al-Saidi and A. M. Rappe, Phys. Rev. B **82**, 155304 (2010).
[27] A. M. Rappe, K. M. Rabe, E. Kaxiras, and J. D. Joannopoulos, Phys. Rev. B Rapid Comm. **41**, 1227 (1990).
[28] http://opium.sourceforge.net.
[29] K. Momma and F. Izumi, Journal of Applied Crystallography **41**, 653 (2008).
[30] M. Stengel, P. Aguado-Puente, N. A. Spaldin, and J. Junquera, Phys. Rev. B **83**, 235112 (Jun 2011).
[31] M. Mrovec, J.-M. Albina, B. Meyer, and C. Elsässer, Phys. Rev. B **79**, 245121 (2009).
[32] A. Baldereschi, S. Baroni, and R. Resta, Phys. Rev. Lett. **61**, 734 (1988).
[33] P magnitudes are evaluated using the ratio of the Ti displacements in the middle of $PbTiO_3$ film to those in the bulk-$PbTiO_3$.
[34] A. M. Bratkovsky and A. P. Levanyuk, Phys. Rev. Lett. **94**, 107601 (2005).

DRAFT